WPJET4 Gamma Camera Upgrade (GCU)

D09	Pilot spectrometer N1

Replacing the existing Gamma-ray detectors of the camera for improving the energy resolution and count rate capability needed for operation in the DT campaign. Target values are an energy resolution of 5% at 1.1 MeV and a count rate capability exceeding 500 kHz.

To design the best photon detector replacing the existing CsI:Tl scintillators coupled to Si PiN photodiode, three different sensitive light detection devices are taken into account: photodiode (PiN diode), Photomultiplier Tubes (PMTs) and Multi Pixel Photon Counter (MPPC). Results from studies committed to a system based on photodiodes and photomultiplier tubes were presented in the D07 GCU report „Evaluation of compact photon detector: compact photomultiplier tubes, photodiodes".

This report summarizes results obtained for the N1 pilot spectrometer based on CeBr3 scintillators coupled to MPPC. Measurements were performed at both NCBJ and JET (May and October 2015).

Due to this very strong voltage-temperature dependence for MPPC-based detectors, a device for real-time temperature monitoring and MPPC gain stabilization was designed and produced at NCBJ. The MPPC Temperature Compensation Device (MTCD@NCBJ) is using a measured dependence of a bias voltage on temperature to maintain a constant value of the MPPC gain. MTCD@NCBJ provides a current limitation and filtering of the MPPC bias voltage and can supply an output voltage up to 80 V. All functions are controlled from a personal computer. More details about MTCD can be found in [I.Zychor et al., High performance detectors for upgraded gamma ray diagnostics for JET DT campaigns, accepted for publication in Physica Scripta].

The NCBJ team installed at JET in May 2015 two detectors: Φ20x20 and Φ20x15 mm CeBr3 scintillators coupled to a 12x12 mm MPPC photo-detector, Hamamatsu model S12642-0404PB-50. They are mounted in channel 9 and 10 in the horizontal part of the JET Gamma Camera, respectively, see photos below.

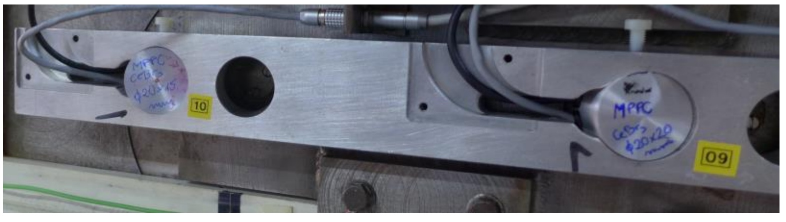

First measurements were performed with two gamma-ray standard sources, ^{137}Cs and ^{22}Na. These sources are characterized by relatively low activity. Unfortunately, an AmBe source could not be used due to problems at JET.

We used a CAEN DT5720 digitizer to register energy spectra.

Finally, we received two signals from each detector ($CeBr_3$+MPPC):

1. output signal from MPPC-based detector,
2. information from a temperature sensor mounted on a PCB board in a capsule with MPPC.

In Fig. 1 a signal registered with a setup based on a $CeBr_3$ scintillator coupled to MPPC, without using the MTCD, is shown. An “after pulse” structure is observed because an existing JET 75 Ω coaxial cable of a length 80 m was used. Our electronics works with 50 Ω termination and using 75 Ω caused the “after pulse” signal.

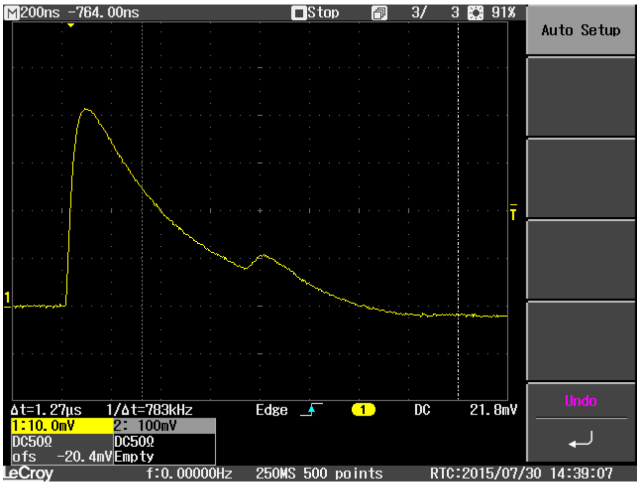

Fig. 1. Signal registered with a $CeBr_3$ crystal (channel 9) coupled to MPPC but without MTCD. An “after pulse” structure is observed because a JET 75 Ω coaxial cable of a length 80 m was used.

In Fig. 2 the signals registered with the same setup as above described but with a MTCD device in operation are presented for two different time scale per division: 20 µs (Fig. 2a) and 5 µs (Fig. 2b).

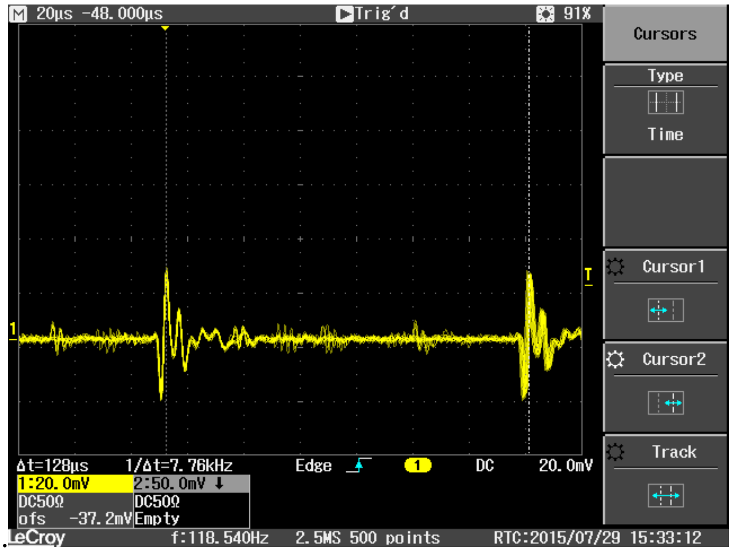

Fig. 2a. Signal registered at JET. Time scale: 20 µs per division.
A noise is seen with different amplitudes and occurring at different frequency.

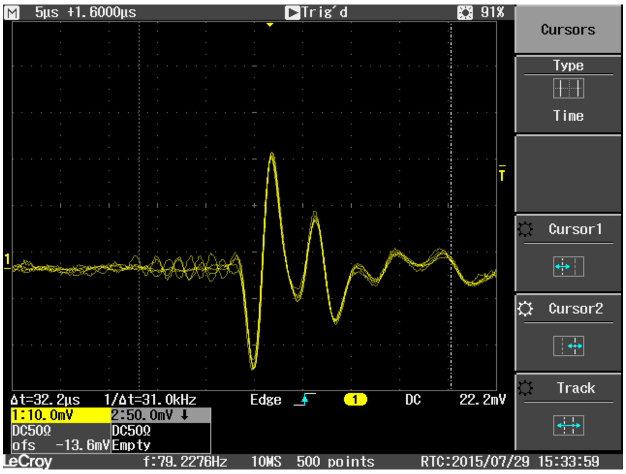

Fig. 2b. The structure of noise, from above measured spectrum, at time scale: 5 µs per division.

With the MTCD@NCBJ in operation, strong oscillations were then observed with an amplitude comparable to observed for a signal from a MPPC-based detector without MTCD, see Fig. 1.

In Fig. 3 spectra registered with and without MTCD are shown. In both cases, ^{137}Cs and ^{22}Na sources were used simultaneously. Both spectra were recorded during the same time equal to 4000 seconds and under the same experimental conditions, including gains and bias voltage. Much higher statistics in the spectrum shown in the upper part in Fig. 3 is caused by noise as observed in the signal in Fig. 2. In this case it is not possible to extract physical peaks originating from calibration sources, as seen in the lower part in Fig. 2. Using calibration sources with much higher activity should allow us to observe peaks above the noise level.

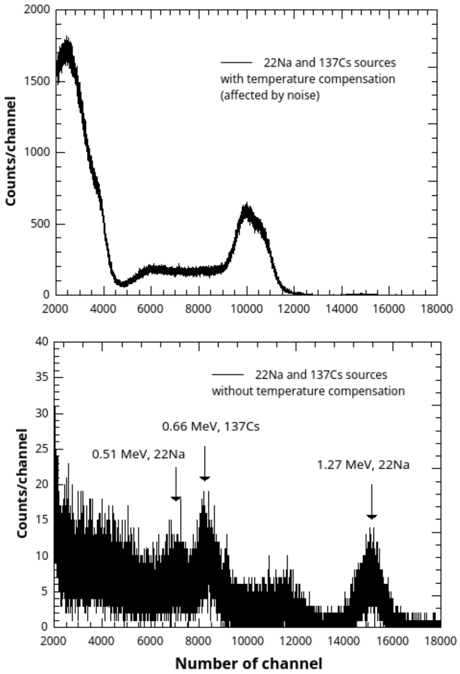

Fig. 3. Energy spectrum of ^{137}Cs and ^{22}Na (two sources used simultaneously). Upper part: a measurement with MTCD, lower: no MTCD in use. Measuring time: 4000 s.

We suspect that observed oscillations, in both time and energy spectra, are connected with a cabling to a temperature control system because disconnecting the MTCD device removed oscillations.

It is worth noting, that these oscillations were not observed during our previous visit at JET with MTCD connected without 80 m long cables – the rest of setup was the same.

Due to problems described above, we decided to continue measurements without MTCD.

Fig. 4. presents energy spectra of ^{137}Cs and ^{22}Na measured for both MPPC-based detectors installed at JET in channels 9 and 10. Operating voltage for both detectors was 65.8 V and a live time of measurement was 58600 s (~16 hours).
We can observe a clear structure with peaks at 0.66 MeV from ^{137}Cs, 1.27 MeV from ^{22}Na and 2.61 MeV from ^{208}Tl. The 2.61 MeV line comes from background from thorium chain. A line with energy of 0.511 MeV from ^{22}Na is not so evident due to a complicated structure in this energy range (full energy peak + Compton edge from ^{137}Cs).
Measured temperature change before and after data collection was equal to 0.2°C.

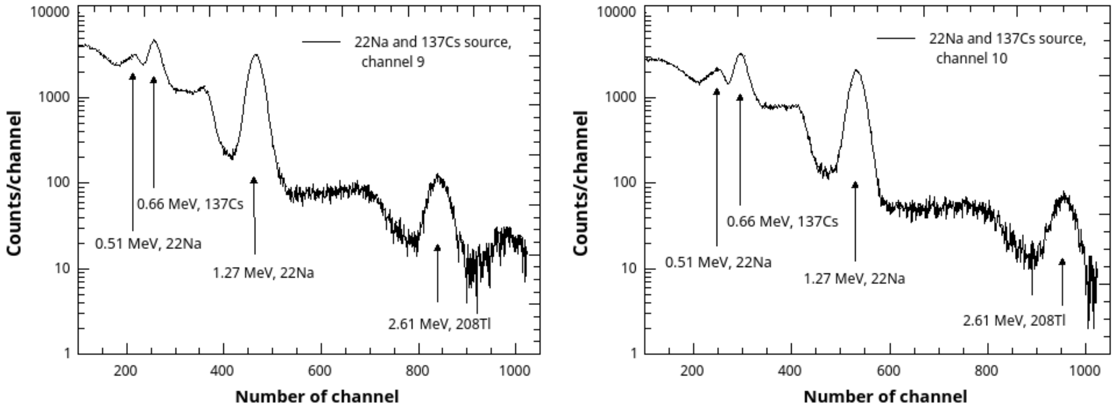

Fig. 4. Energy spectrum of ^{137}Cs and ^{22}Na registered with MPPC-based detectors located in channel 9 and 10.

In the same time we managed to register an energy spectrum from channel 5, based on CsI scintillator and PIN diode, see Fig. 5.
To collect this data we used TUKAN-8K channel analyzer. Live time of measurement was comparable with this performed for MPPCs with a CAEN digitizer (58200 s). Collected data allow us to compare energy resolution and estimate real temperature influence for FWHM parameter. Numerical data for 1.27 MeV line of ^{22}Na are presented in table 1.

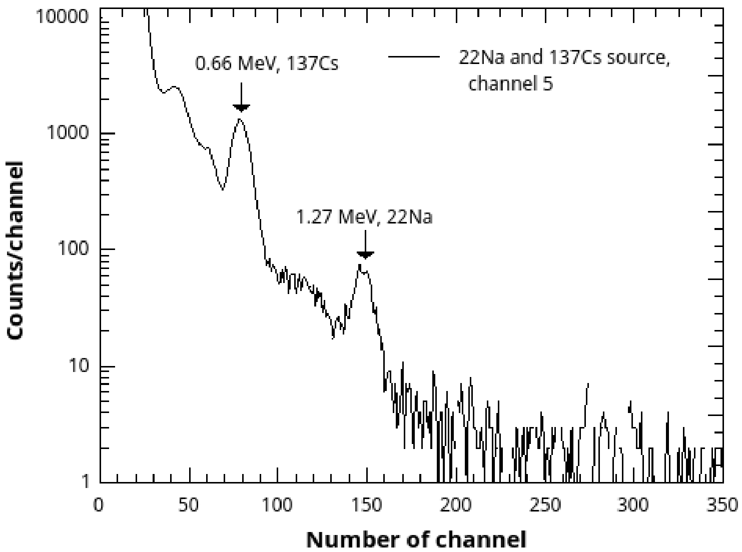

Fig. 5. Energy spectrum of ^{137}Cs and ^{22}Na measured for an CsI-based detector located in channel 5.

Table 1. Energy resolution obtained for 1.27 MeV line of ^{22}Na for CsI based detector (channel 5) and both MPPC based detectors (channels 9 and 10).

Number of channel	scintillator	FWHM [%]
5	CsI + PiN diode	7.10+/-0.17
9	20×20 mm $CeBr_3$ + MPPC	7.00+/-0.19
10	20×15 mm $CeBr_3$ + MPPC	6.50+/-0.15

Our conclusions
- temperature changes in a final position of GCU detectors are small, especially during short period time,
- no FWHM worsening observed during long day-night measurement.

During our visit at JET in October 2015 we continued tests of gamma-ray detector based on a 12x12 mm MPPC photo-detector coupled to $CeBr_3$ scintillator, already installed at JET. Each time the output signals were transmitted through a 108 m long cable type L300 (75 Ω impedance).

Due to the mismatch of the impedance of the cable type L300 (R_c = 75 Ω), short coaxial cables (R_c = 50 Ω) and the acquisition system (R_s = 50 Ω) after-pulses were observed. Reflected signals were delayed about 0.7 µs in reference to main pulses. Structure of this kind of signals, registered for 22Na with 50 Ω terminated oscilloscope, is presented in Fig. 6.

To minimize observed reflection we decided to change short coaxial cables between the J1D cubicle and the KN3G digitizer board to new ones with impedance 75 Ω. The termination of KN3G digitizer was also changed to this value. The signal registered after these modifications is presented in Fig. 7.

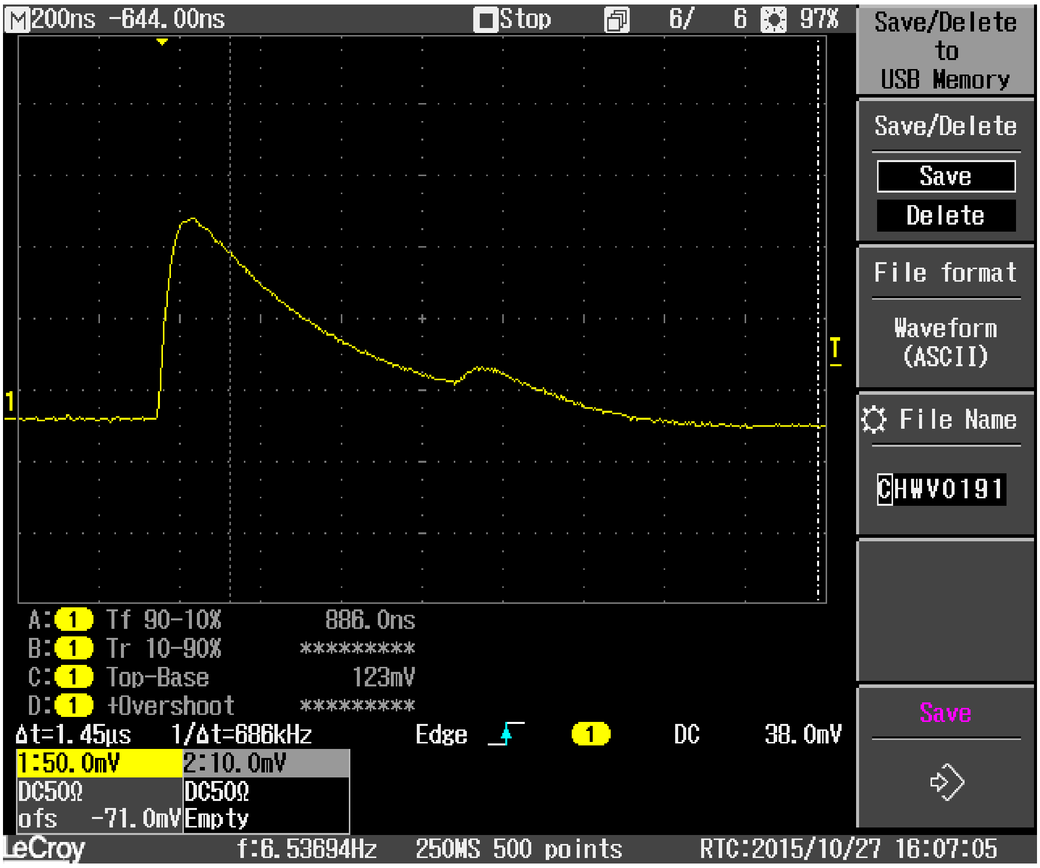

Fig. 6. Example of signal from MPPC based detector (ch 9) registered for 22Na gamma source. Signal length rise time is ~40 ns and fall time ~890 ns. After-pulse structure is observed after ~700 ns from the maximum

of main component.

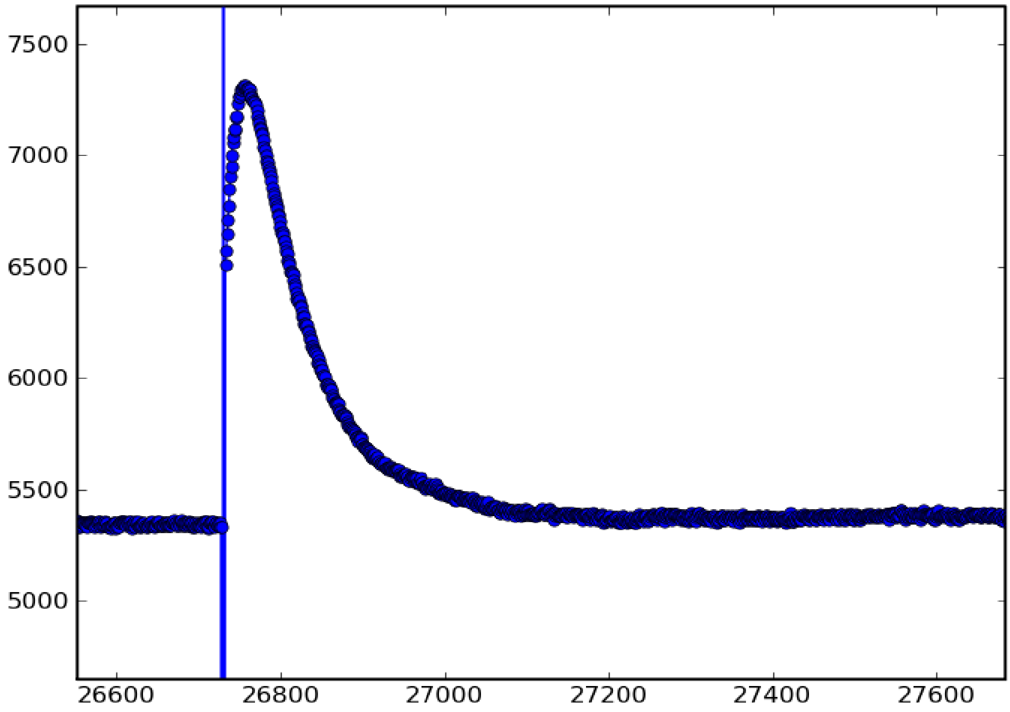

Fig. 7. Signal form MPPC based detector (ch 9) registered by KN3G digitizer. Digitizer was terminated by 75 Ω. Signals between J1D cubicle and KN3G digitizer were derived by 75 Ω coaxial cable. Single bin size corresponds to 5 ns length. Total length of the pulse is ~1.8 µs.

Tests of signal shortening with the CR differential circuit.

To check the possibility of signal shortening at JET, the CR differential circuit was prepared at NCBJ . In our laboratory we managed to reduce signal length from 1.2 µs to ~120 ns and tested it successfully for a counting rate below 300 kHz. It needs to be highlighted, that all our tests were performed for the impedance of 50 Ω, including cabling, connectors and digitizer termination.

Due to the limited access to installed prototype detectors, we decided to mount the CR circuit after the 108 m long cable (type L300) in the J1D cubicle and before the KN3G digitizer (see Fig. 8). The best parameters obtained for the CR circuit in NCBJ were chosen as initial values at JET (R=750 Ω and C=820 pF, respectively).

First tests of signal shortening were done with a 50 Ω terminated oscilloscope (no 75 Ω termination option). Print screens for this case are presented in Fig. 9 and Fig. 10. As we can see, we managed to reduce signal length to ~26 ns rise time (10-90%) and 187 ns fall time (90-10%) but we still saw strong reflections in the region of after-pulse (after ~0.7 µs).

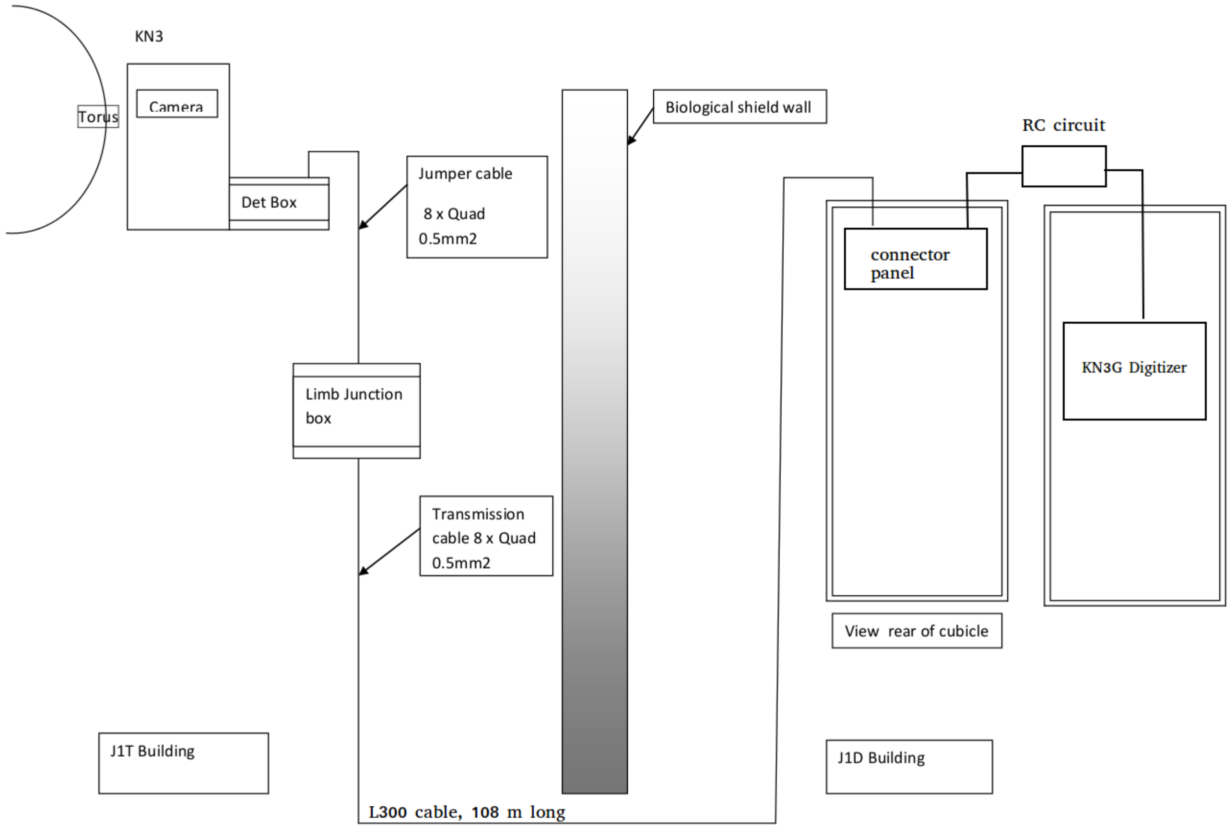

Fig. 8 Schematic view of the CR circuit location at JET facilities.

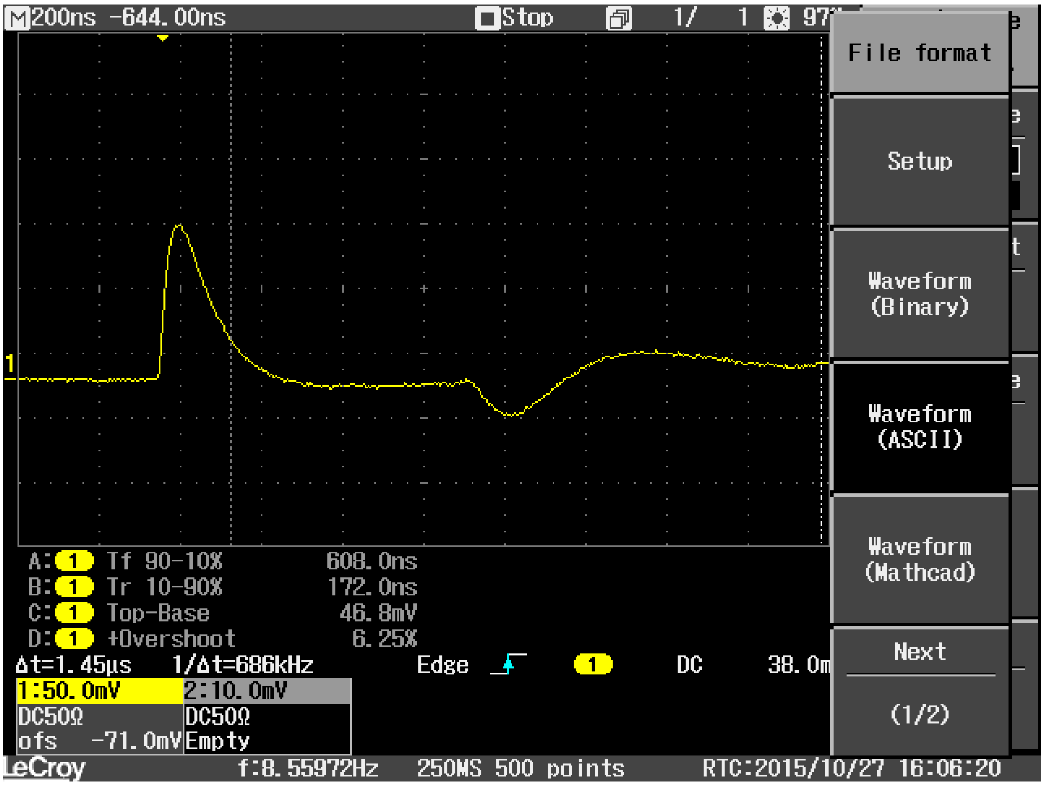

Fig. 9. Signal length after using the CR circuit. Best parameters in this case were obtained for resistor R=750 Ohm and capacitor C=820 pF. Main component rise time (10-90%) is equal ~26 ns, fall time (90-10%) ~187 ns (see also Fig. 10.). Under- and overshoot in the region of the after-pulse (see Fig. 6.) is observed.

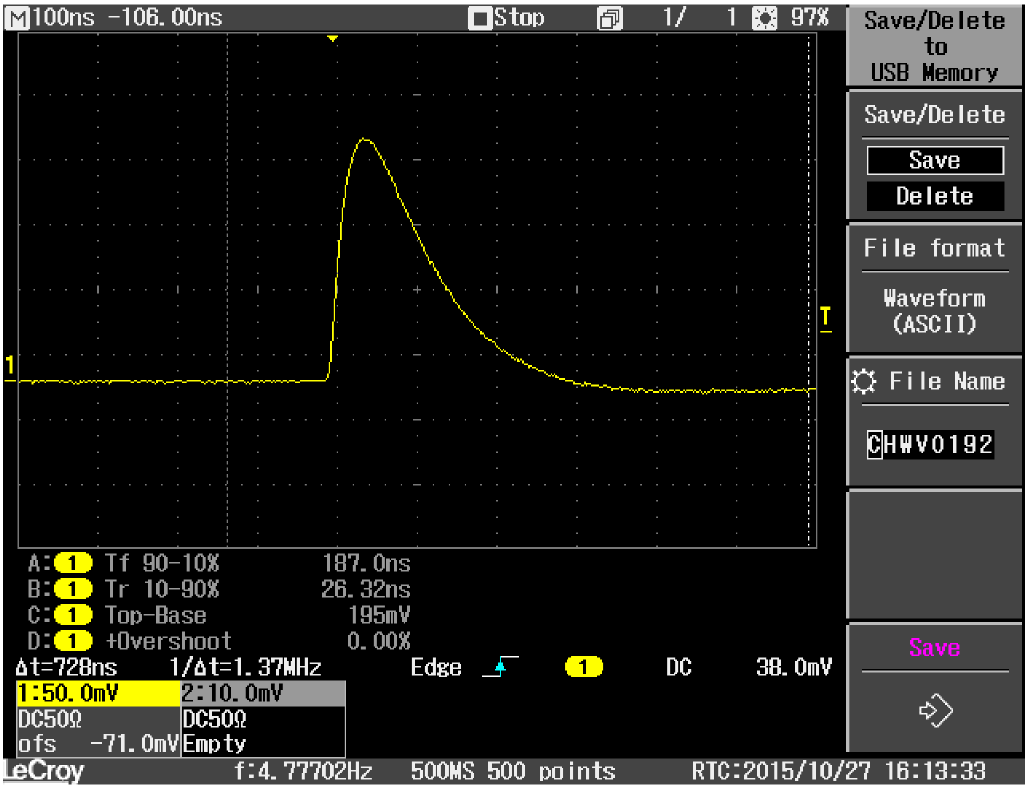

Fig. 5. Zoom in on the main component of the signal after using the CR circuit.

In the next step we registered shortened by the CR circuit signals directly by the KN3G digitizer. We tested different combinations of resistors for two sets of capacitors: C=820 pF and C=3.3 nF. Figures below present the shape of obtained pulses.

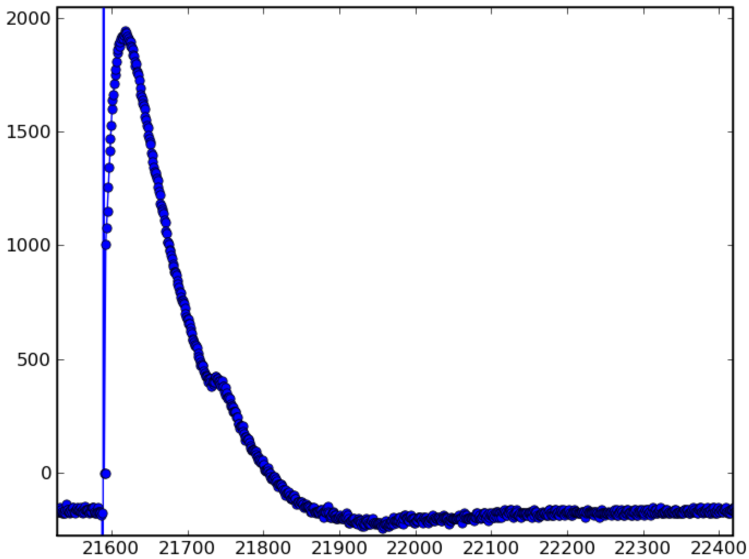

C=820 pF,R=750 Ω

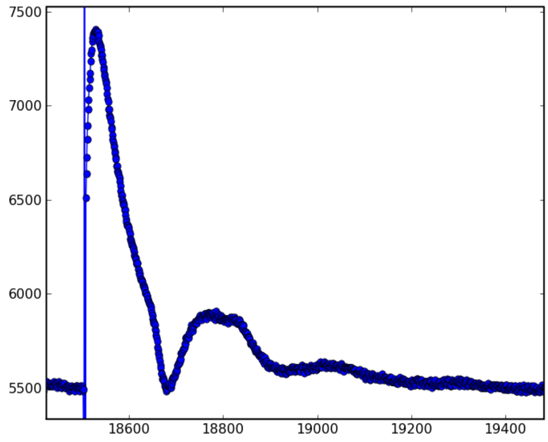

C=820 pF, R= 96 Ω

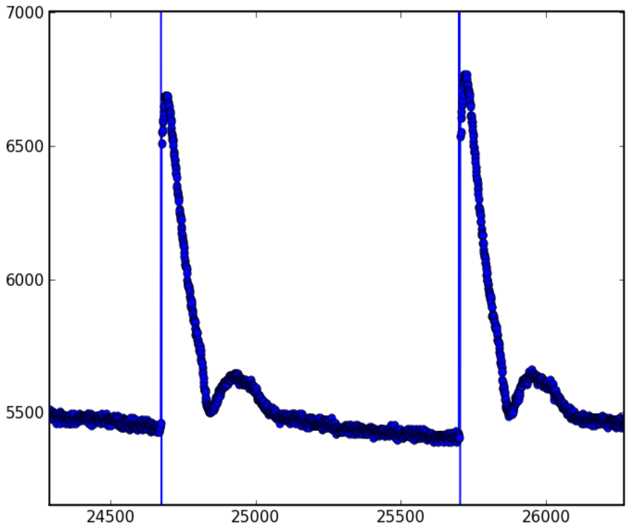

C=820 pF, R=50 Ω

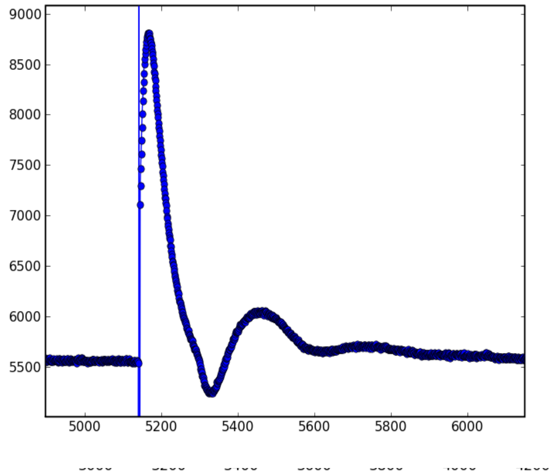

C=820 pF, R=25 Ω

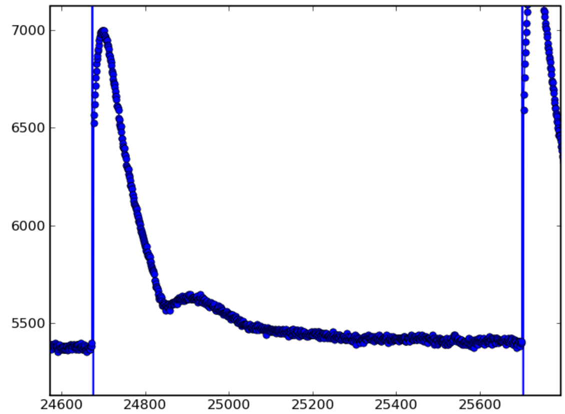

C=3.3 nF, R = 1000 Ω

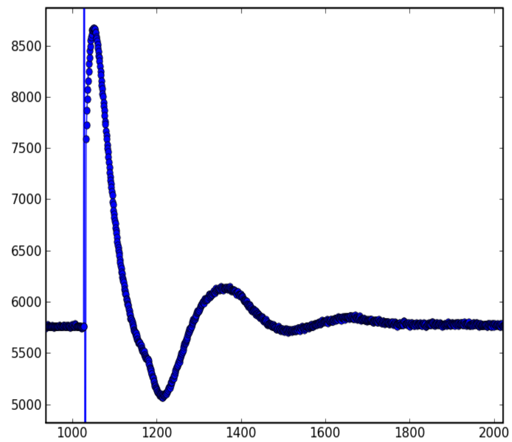

C=3.3 nF, R = 470 Ω

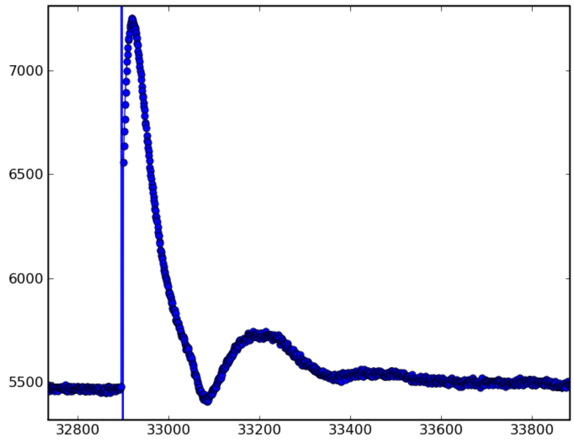

C=3.3 nF, R = 160 Ω

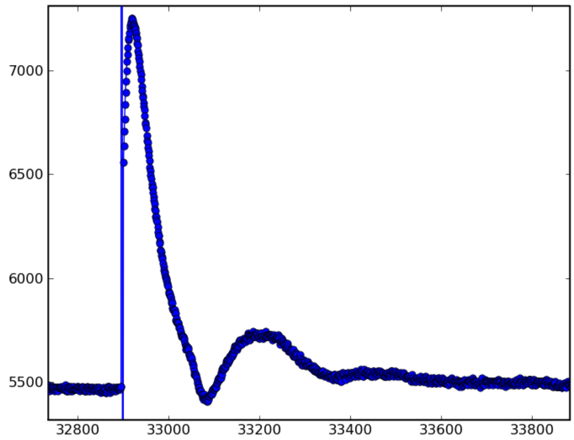

C=3.3 nF, R = 96 Ω

As we can see, we managed to eliminate the undershoot of the pulse, but the overshoot was still present. For better matching of total resistance to 75 Ω, we modified the CR circuit to the one presented in Fig. 19. The best result, including signal shortening, was obtained for R1 = 1000 Ω, C=820 pF and R2 = 80 Ω. After-pulse structure was reduced but not eliminated, see Fig. 20.

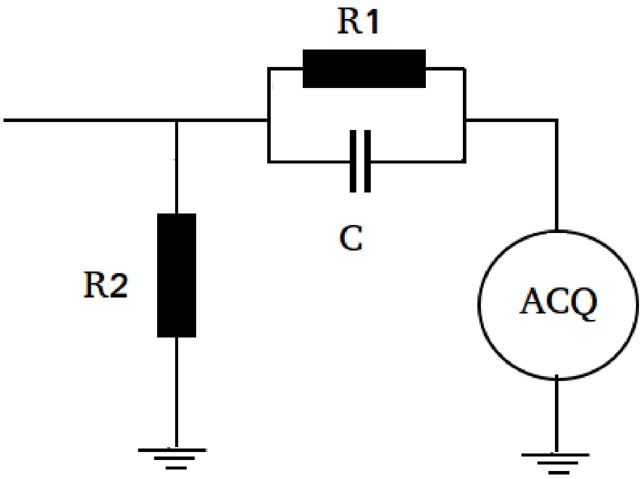

Fig. 19. The CR circuit after modification. R2 was set to get 75 Ω of total impedance.

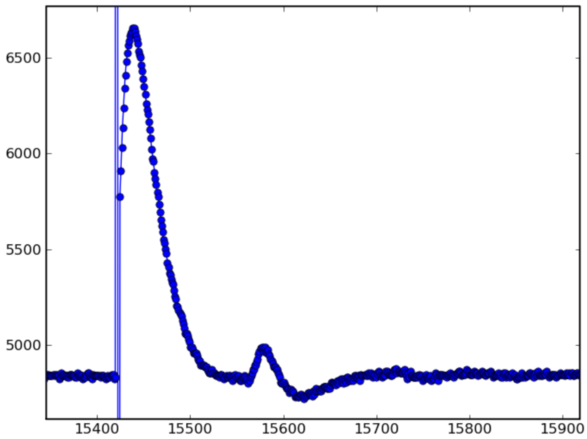

Fig. 20. Signal structure obtained for R1 = 1000 Ω, C=820 pF and R2 = 80 Ω. Single bin corresponds to 5 ns.

Measurements with ^{22}Na and AmBe source.

Due to the non-linearity of the MPPC, the energy calibration in a wide range is needed. We measured gamma energy spectra of $_{22}$Na and AmBe sources for channel 9. To simplify, we were working without the CR circuit. Obtained spectra are presented in Fig. 21. Because of different gains in channels 1 and 3 of the KN3G digitizer, gamma energy spectrum of 22Na was rescaled and adjusted to those from the AmBe source. The line 0.511 MeV, which is present in both spectra, was used as a reference point. This operation allows us to add an extra point (1.274 MeV line) in our calibration. Fig. 22 shows analyzed data and the non-linearity of MPPC based detectors. We observe good linearity only in energy range up to ~ 1.3 MeV. Above this level linearity is not maintained, so the energy of physical peaks cannot be estimated by simple extrapolation, like it was possible for CsI based detectors coupled to PIN diodes. Better accuracy of calibration may be obtained with a longer measurement time for both sources. Moreover additional calibration points can be added from natural background: 1.4 MeV from 40K and 2.6 MeV from 208Tl. These kinds of measurements should be done in the future.

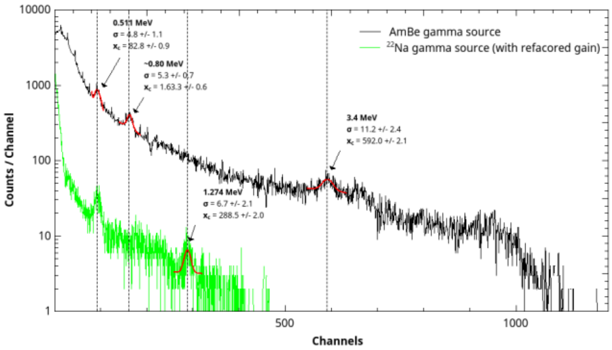

Fig 21. Gamma energy spectrum of AmBe and 22Na. Both spectra from channel 9 were registered with the KN3G digitizer. Due to different gain for both channels of the KN3G digitizer, 22Na energy spectrum was rescaled. As a reference point the 0.511 MeV line was used. Red lines correspond to fitted Gaussian functions. For each peak centroid and width (1 sigma) with one standard deviation value was obtained.

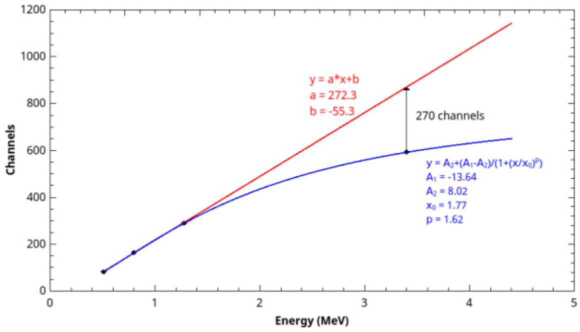

Fig. 22. The non-linearity in the energy scale of a MPPC based detector. Calibration points (black circles) were obtained for identified peaks in Fig. 21. Red line corresponds to linear fit based on first three points (range of 0.511 – 1.274 MeV). Blue curve is described by an arbitrary chosen equation for better following the trend of data points.

Tests of the triggering system for MTCD@NCBJ

During our visit we also managed to make tests of the new triggering system for the temperature compensation device, see previous report from our visit at JET. Previous measurements showed that during the temperature readout, noise comparable to the amplitude of the correct signal is generated in the 108 m long signal cable. Due to these problems we decided to resign from a continuous monitoring of the temperature. Our idea was to measure the temperature for a short period of time, after getting the triggering signal from CODAS and before the plasma shot. Based on these short measurements, the bias voltage for MPPC based detectors will be set.

The triggering signal was correctly accepted by hardware. The new version of firmware for MTCD@NJCB is under development.

Conclusions

- A signal shortening method based on the CR circuit does not work as good as at NCBJ at the end of L300 cable. At JET the shortest obtained signal length is about 500 ns, at NCBJ – 120 ns.
- Results presented above can be improved by modification of the printed circuit board for MPPC, already installed at JET in channel 9 and 10, but the access to the horizontal camera is needed.
- TIA, still under development, as an alternative solution for signal shortening must be tested at JET. The access to the horizontal camera is necessary in this case.
- To eliminate the after-pulse structure, see Fig. 20, a correct matching of system impedance (75 Ω) is needed, including cables and the acquisition system – a close collaboration with Ana and JET is needed.
- If the after-pulse structure is not eliminated, a new algorithm of off-line analysis must be prepared for DAQ.
- Hardware for the triggering system of MTCD@NCBJ was positively tested at JET, software is under development.
- Due to the non-linearity of MPPC, the energy calibration in a wide energy range for each detector should be done after installation at JET.
- Internal gain in the KN3G digitizer should be adjusted to the prototype detectors and the energy range expected in the DT campaign.

The report was prepared by the NCBJ team
Grzegorz Bołtruczyk, Andrzej Brosławski, Marcin Gosk, Stefan Korolczuk,
Sławomir Mianowski, Izabella Zychor.

The present document is of intellectual property of the JET Enhancements (JET4) Work Package (in particular NCBJ_IPPLM). This document cannot be neither copied nor distributed without right permission from EUROfusion Consortium.
This scientific work was partly supported by Polish Ministry of Science and Higher Education within the framework of the scientific financial resources in the years 2015-2017 allocated for the realization of the international co-financed project.
This work has been carried out within the framework of the EUROfusion Consortium and has received funding from the Euratom research and training programme 2014-2018 under grant agreement No 633053. The views and opinions expressed herein do not necessarily reflect those of the European Commission.